

## Universal control of nuclear spins via anisotropic hyperfine interactions

J. S. Hodges, J. C. Yang, C. Ramanathan, and D. G. Cory

Department of Nuclear Science and Engineering, Massachusetts Institute of Technology, Cambridge, Massachusetts 02139, USA

(Received 31 July 2007; published 8 July 2008)

We propose a method for completely controlling a nuclear spin subsystem using only microwave irradiation of resolved anisotropic hyperfine interactions with a single electron spin. This paradigm of control has important applications for spin based solid-state quantum information processing. In particular we argue that indirect addressing of the nuclear spins via an electron spin acting as a spin actuator allows for nuclear spin quantum logic gates whose operational times are significantly faster than either gates based on rf fields resonant with nuclear spin flips or nuclear-nuclear dipolar interactions. We demonstrate experimental aspects of this method with one electron and one nuclear spin of a single crystal of irradiated malonic acid.

DOI: 10.1103/PhysRevA.78.010303

PACS number(s): 03.67.-a, 76.30.-v, 76.60.-k

### I. INTRODUCTION

Coherent control of quantum systems promises optimal computation, secure communication, and new insight into the fundamental physics of many-body problems. Solid-state proposals [1,2] for such quantum information processors employ isolated spin degrees of freedom which provide Hilbert spaces with long coherence times. Of particular interest are hybrid systems of electron and nuclear spins. Here a single electron spin provides a means for state preparation and qubit readout while the nuclear spins act as qubits for storing and processing information. Coherent control has recently been demonstrated in several hybrid physical systems including organic [3] and inorganic [4] single crystals, phosphorous donors in Si [5], endohedral fullerenes [6,7], and nitrogen-vacancy centers in diamond [8–11].

Here we present a method for controlling an electron-nuclear system without explicitly relying on nuclear spin Rabi oscillations. Our method extends the techniques developed for electron spin envelope echo modulation, such as nuclear spin [12] and coherence transfer [13] echoes. We use the anisotropy of the hyperfine interaction along with optimal control methods developed for quantum information processing (QIP) to generate arbitrary quantum gates while addressing only the electron spin. This approach provides a fast and reliable means of controlling nuclear spins and enables the electron spins of such solid-state systems to be used for state preparation and readout of nuclear spin states. In addition, we describe the use of the electron as a *spin actuator* [14] for mediating nuclear-nuclear spin gates.

### II. MODEL SYSTEM

The spin Hamiltonian of a single localized electron spin with angular momentum,  $S=1/2$  and  $N$  nuclear spins, each with angular momentum  $I^k=1/2$ , in the presence of a magnetic field  $\vec{B}$  is [15]

$$\mathcal{H} = \beta_e \mathbf{g}_{\mu\nu} \hat{S}_\mu B_\nu - \sum_{k=1}^N \gamma_n^k (1 - \delta_{\mu\nu}^k) \hat{I}_\mu^k B_\nu + 2\pi \sum_{k=1}^N \mathbf{A}_{\mu\nu}^k \hat{S}_\mu \hat{I}_\nu^k + \pi \sum_{k,l=1}^N \mathbf{D}_{\mu\nu}^{kl} \hat{I}_\mu^k \hat{I}_\nu^l. \quad (1)$$

Here  $\beta_e$  is the Bohr magneton,  $\gamma_n^k$  is the gyromagnetic ratio;  $\hat{S}$  and  $\hat{I}^k$  are the spin-1/2 operators. The second-rank tensors  $\mathbf{g}$ ,  $\mathbf{A}^k$ ,  $\delta^k$ , and  $\mathbf{D}^{kl}$  represent the electron  $g$  factor, the hyperfine interaction, the chemical shift, and the nuclear dipole-dipole interaction respectively. In the regime where the static magnetic field  $\vec{B}=B_0\hat{z}$  provides a good quantization axis for the electron spin, the Hamiltonian can be simplified by dropping the nonsecular terms, keeping only electron interactions involving  $S_z$ . The quantization axis of any nuclear spin, however, depends on the magnitudes of both the hyperfine interaction and the static magnetic field, as well as their relative orientations. When these two fields are comparable in magnitude  $\mathcal{H}$  is well approximated as

$$\mathcal{H}_0 \approx \beta_e g_{zz} B_0 \hat{S}_z - \sum_{k=1}^N \gamma_n^k (1 - \delta_{zz}^k) B_0 \hat{I}_z^k + 2\pi \sum_{k=1}^N (A_{zx}^k \hat{S}_z \hat{I}_x^k + A_{zy}^k \hat{S}_z \hat{I}_y^k + A_{zz}^k \hat{S}_z \hat{I}_z^k)$$

[16]. The nuclear dipole-dipole interaction is neglected as it is at least 100 times weaker than the hyperfine terms.

Any nuclear spin in this regime is quantized in an effective field that is the vector sum of the Zeeman and hyperfine interaction (Fig. 1). Its eigenstates are a mixture of the nuclear Zeeman eigenstates:  $|\alpha_0\rangle = \cos\theta_{\uparrow} |\uparrow\rangle + e^{i\varphi} \sin\theta_{\uparrow} |\downarrow\rangle$ .  $|\alpha_1\rangle$  is orthogonal to  $|\alpha_0\rangle$ .  $\theta_{\uparrow,\downarrow}$  and  $\varphi$  are determined geometrically:  $\tan(\theta_{\uparrow,\downarrow}) = -\frac{A_{\perp}}{A_{zz} \pm \omega/\pi}$  and  $\varphi = \arctan(A_{zy}/A_{zx})$ . An  $N$ -bit string of quantum information can be stored in this system in either the spin-up or spin-down electron manifold. In the spin-up case, the state is

$$|j_1 j_2 \cdots j_N\rangle = |\uparrow\rangle \otimes |\alpha_{j_1}^1\rangle \otimes |\alpha_{j_2}^2\rangle \otimes \cdots \otimes |\alpha_{j_N}^N\rangle, \quad (2)$$

where  $j_k \in \{0, 1\}$ . Note that by storing information in either the  $|\uparrow\rangle$  or  $|\downarrow\rangle$  electron spin manifolds there is no spin superposition of the electron wave function and the electron spin remains separable from the nuclear spins.

### III. UNIVERSAL CONTROL OF $2^{N+1}$ -DIMENSIONAL HILBERT SPACE

The necessary and sufficient conditions for complete controllability, or universality, are that the nested commutators of the natural Hamiltonian ( $\mathcal{H}_N$ ) and each of the control

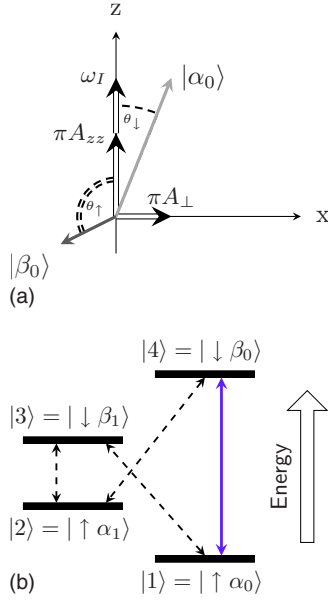


FIG. 1. (Color online) (a) The electron spin state is aligned (or antialigned) with the quantization axis given by  $\vec{B}=B_0\hat{z}$ , while the nuclear spin state aligns along the local field. When the electron spin is  $|\uparrow\rangle$ , the nuclear spin quantization axis,  $|\alpha_0\rangle$  is a vector sum of  $A_{zz}$ ,  $\omega_I$  along  $\hat{z}$  and  $A_{\perp}$  along  $\hat{x}$  drawn as double arrows. ( $A_{\perp}=\sqrt{A_{zx}^2+A_{zy}^2}$ ). When the electron spin is  $|\downarrow\rangle$ , the sign of  $A_{zz}$  and  $A_{\perp}$  is negative, yielding a different nuclear quantization axis  $|\beta_0\rangle$ . (b) Since  $\langle\beta_m|\alpha_l\rangle\neq 0$ , electron spin flips induced by the  $\hat{S}_x$  operator drive many transitions (dashed arrows) between energies of  $\mathcal{H}_0$ . This allows for universal control of the entire spin system. In our experimental setup ( $N=1$ ) the energy differences are  $\omega_{12}/2\pi=7.8$  MHz,  $\omega_{34}/2\pi=40$  MHz,  $\omega_{14}/2\pi=12.005$  GHz,  $\omega_{23}/2\pi=11.954$  GHz.

Hamiltonians ( $\{\mathcal{H}_C\}$ ) form a closed Lie group  $SU(2^{N+1})$  [17,18]. An equivalent diagrammatic representation [19,20] relies on graph connectivity for assessing the controllability of quantum systems represented as Lie algebras. Altafini [19] has shown that barring degenerate eigenvalues  $E_l$  of  $\mathcal{H}_N$  or degenerate transition frequencies ( $\hbar\omega_{lm}=E_l-E_m$ ), the matrix representation of  $\mathcal{H}_N$  is strongly regular. This condition along with the complete connectivity of the graph generated by the matrix elements of  $\mathcal{H}_C$  guarantees universality.

In the anisotropic hyperfine coupled electron-nuclear system both of these conditions are satisfied. The classical controls are time-dependent microwave fields oscillating at the electron spin resonance frequency ( $\sim\beta_e g_{zz} B_0$ ) and parametrized by three values:  $B_1^e$ , the amplitude of an oscillating magnetic field ( $\perp B_0\hat{z}$ );  $\Omega$  the frequency of oscillation; and  $\phi$  the phase of the oscillation. This yields the control Hamiltonian:

$$\mathcal{H}_C(B_1^e, \Omega, \phi) = \beta_e g_{zz} B_1^e(t) \{ \cos[\Omega t + \phi(t)] \hat{S}_x + \sin[\Omega t + \phi(t)] \hat{S}_y \}.$$

The connectivity of the eigenstates by  $\mathcal{H}_C$  is determined by drawing an edge between the  $|l\rangle$  and  $|m\rangle$  states if  $\langle l|\mathcal{H}_C|m\rangle\neq 0$ . Since  $\mathcal{H}_0$  only contains  $\hat{S}_z$  terms it is block-

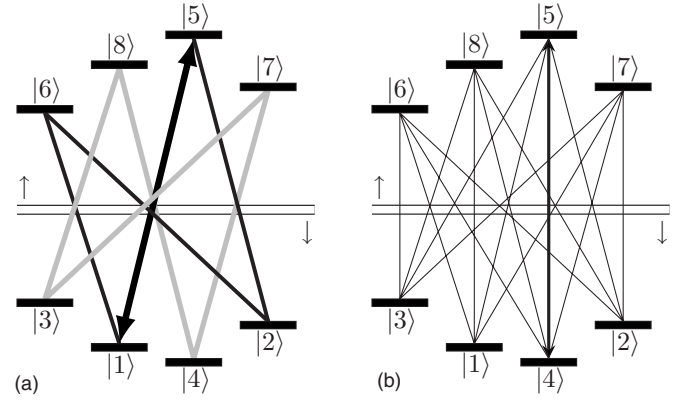


FIG. 2. The connectivity of energy levels of  $1e-2n$  system. When the control Hamiltonian is applied resonant with a single transition (bold line) it excites detuned transitions between the levels of the electron spin up and spin down manifolds (double line). An edge is drawn between two eigenstates if the control Hamiltonian operator has a nonzero matrix according to  $[\langle m|\hat{S}_x|l\rangle\neq 0]$ . (a) If one of the hyperfine tensors between a nuclear spin is isotropic, universality does not occur. The control operator induces transitions that join two sets of four levels (gray and black), but does not join all levels. (b) Full connectivity is achieved when both hyperfine interactions are anisotropic.

diagonal with orthogonal electron spin subspaces  $|\uparrow\rangle$  and  $|\downarrow\rangle$ . The  $2^N$  states for the  $\uparrow$  manifold are given by Eq. (3); for the  $\downarrow$  manifold they are  $|p_1\dots p_N\rangle=|\downarrow\beta_{p_1}^1\dots\beta_{p_N}^N\rangle$ . Thus, all transitions changing the electron spin states are allowed by  $\mathcal{H}_C$ . For these states  $\langle p_1\dots p_N|\mathcal{H}_C|j_1\dots j_N\rangle=\prod_{k=1}^N\langle\beta_{p_k}|\alpha_{j_k}\rangle$ . From Fig. 1(a), it is clear that as long as  $A_{\perp}^k\neq 0$ ,  $\langle\beta_{0,1}^k|\alpha_{0,1}^k\rangle\neq 0$ . In this case, any single level in the  $\uparrow$  manifold is connected to all of the  $2^N$  states in the  $\downarrow$  manifold, and vice versa. Regarding the strong regularity of  $\mathcal{H}_0$ , for the  $1e-N$  nuclear spin system, distinct Larmor frequencies (sum of Zeeman and chemical shift) and hyperfine couplings for each nuclear spin guarantee the nondegeneracy of the eigenstates. The hyperfine couplings and the Zeeman frequencies must also be chosen such that  $\omega_{jk}/\omega_{j'k'}\neq 1$ . Figure 2 shows diagrammatic examples for  $N=2$ ; it shows that universal control over a set of nuclear spins, each with an anisotropic hyperfine coupling, is obtained with only an amplitude modulated wave form applied to any electron spin transition at a fixed  $\Omega$ .

We can provide some insight into how modulation of the electron spin state through shaped microwave fields provides control over the nuclear spins. Flipping the electron spin changes the quantization axis of the nuclear spins. Since these two quantization axes are separated by a large angle, a sequence of spin evolutions under these two noncommuting axes permits arbitrary nuclear rotations. If we consider collective motions of the  $N$  nuclear spins relative to the two electron spin states, this generates the complete algebra in  $SU(2^{N+1})$ . Given the complexity of the full dynamics of these  $2^N$  vectors, we can use numerical optimal control methods developed for and applied to nuclear magnetic resonance QIP in order to engineer arbitrary unitaries [21–23]. By limiting the control fields of the electron-nuclear system to only the electron spin flip transitions we achieve quantum gates

whose operation times are faster than if we had relied upon nuclear spin nutation rate alone [7,24].

#### IV. 1e-1n SYSTEM

We demonstrate the utility of this control scheme by exploring Ramsey fringes [28] in a 1e-1n system—a single crystal of x-ray irradiated malonic acid [29]. The parametrized Hamiltonian is  $\mathcal{H}_0/2\pi = \nu_s \hat{S}_z - \nu_n \hat{I}_z + A_{zx} \hat{S}_z \hat{I}_x + A_{zz} \hat{S}_z \hat{I}_z$ , where  $\nu_s = 11.885$  GHz,  $\nu_n = 18.1$  MHz,  $A_{zx} \approx 14.2$  MHz, and  $A_{zz} \approx -42.7$  MHz. The control Hamiltonian parameters are  $\max[\beta_e g_{zz} B_1^e(t)]/2\pi = 7$  MHz and  $\Omega/2\pi = 11.909$  GHz. No arbitrary phase controls  $\phi(t)$  were used as they are not a necessary element of  $\mathcal{H}_C$  for universal control. All experiments were performed on a home-built pulsed electron spin resonance (ESR) spectrometer and cryogenic probehead with a loop-gap resonator.

#### V. EXPERIMENTAL RESULTS

To make the description more concrete we have used the aforementioned techniques to indirectly observe nuclear precession via an electron spin. While indirect nuclear observation is well known in the magnetic resonance literature [e.g., electron-nuclear double resonance and echo modulation], we present an example where optimal control theory is used to develop control sequences for ESR. To implement an arbitrary unitary propagator we use the gradient ascent pulse engineering (GRAPE) [21] algorithm for finding the control field  $B_1^e(t)$ . Constraints on the modulation sequence, such as maximum nutation rate and pulse bandwidth, were chosen in accordance with our hardware limitations such as finite power amplifiers, modest AWGs, and finite bandwidth components. The simulated gate fidelity [22] of these gates is at least 0.98.

The equilibrium state of the ensemble system,  $\rho_{\text{thermal}} = -\hat{S}_z$ , has no net nuclear spin polarization, so we first transfer the available electron spin polarization to the nuclear spins. This is achieved by selectively inverting the levels  $|2\rangle$  and  $|4\rangle$  or  $|1\rangle$  and  $|3\rangle$  (see Fig. 1 and supporting material). We created coherence between nuclear eigenstates by using a microwave modulation sequence engineered to perform a nuclear  $\pi/2$  pulse selective for only one of the electron manifolds,  $U_{12}(\pi/2)$  [30]. The Ramsey fringe experiment (Fig. 3) measures the phase evolution under  $\mathcal{H}_0$ . We halt the evolution by again applying  $U_{12}(\pi/2)$  and then transferring the polarization back to the electron spin. By monitoring the relative amplitude of the electron spin echo at different times,  $\tau$ , we indirectly observe the nuclear spin dynamics.

Figure 4 shows the coherent oscillations between nuclear coherence on levels  $|1\rangle$  and  $|2\rangle$ . We implement the net unitaries,  $U_{pc} = U_{12}(\pi/2)U_{24}(\pi)$  and  $U_{pc}^{-1}$ , as a single modulation sequence with a total time of 800 ns and simulated fidelities ( $F$ ) 0.99 and 0.98, respectively. All nuclear pulses are achieved through modulation of the hyperfine interaction and are applied resonant with the 1–4 transition. The agreement between the simulated spin system, aligned at  $42.6^\circ$  with respect to the  $c$  axis, and the experimental data points clearly demonstrate an electron spin actuator as we are able to excite

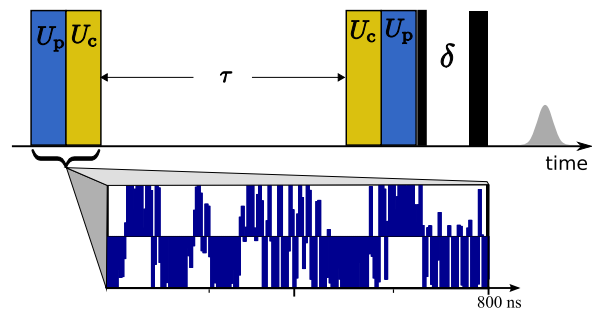


FIG. 3. (Color online) Schematic pulse sequence for measuring Ramsey fringes.  $U_p$  creates a nonequilibrium population difference between levels 1 and 2, and  $U_c$  creates a coherence of the nuclear spin in the  $S = -1/2$  manifold. During  $\tau$ , this coherence evolves under  $\mathcal{H}_0$ , acquiring an observable phase. The coherence is transformed back to a population difference between nuclear spin levels and then to electron spin levels. A pair of short unmodulated pulses are used to detect an electron spin echo whose height is proportional to the resultant electron spin population. The wave form used to implement  $U_p U_c$  is shown in the inset. Note that all pulses have a carrier frequency resonant with the 1–4 transition ( $\Omega/2\pi = 11.909$  GHz) and induce transitions between 1–4, 2–4, 1–3, and 2–3 via time-dependent amplitude modulations.

nuclear spin coherence via GRAPE pulses applied to solely the electron spin.

#### VI. CONCLUSIONS AND OUTLOOK

Using shaped pulse techniques for engineering quantum gates, we have described a method to control nuclear spins coupled via anisotropic hyperfine interactions to a single localized electron spin impurity using *only* electron spin transitions. This proof-of-principle idea has many immediate applications to solid-state quantum information processors. Our

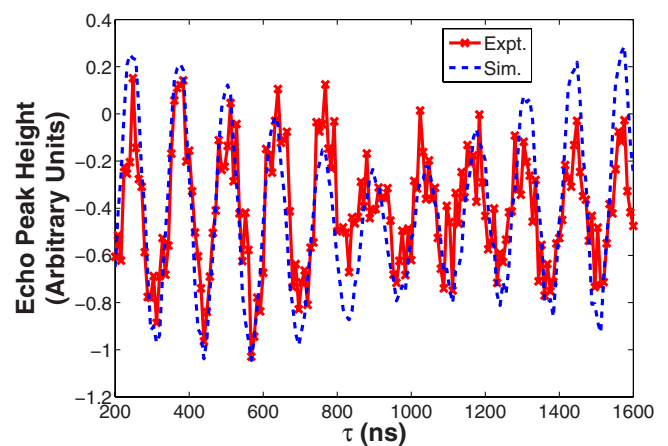


FIG. 4. (Color online) Measurements of the electron spin echo as a function of the time  $\tau$  between coherence transfer indirectly reveal the nuclear precession rate. Numerical simulations of the experiments (solid line) show agreement with the observed signal (dashed). The Ramsey fringe experiment ( $\times$ ) reveals a clear precession of the coherence between the  $|1\rangle$  and  $|2\rangle$  states at roughly 8 MHz.

method extends to any number of nuclear spins that have resolvable anisotropic hyperfine interactions. Simulations of  $1e-2n$  systems show that a complete set of gates over the nuclear subsystem can be easily obtain using the GRAPE algorithm. For example, we have found a  $1e-2n$  controlled-NOT (CNOT) gate [31] between the carbon and proton nuclear spins for malonic acid isotopically labeled with a  $^{13}\text{C}$  at the methylene position. This gate can be performed in only  $2\ \mu\text{s}$ . We note that if only nuclear nutation frequencies and nuclear dipole-dipole interactions were used, such a CNOT would take much longer due to the relative strength of the hyperfine interaction to these nuclear-nuclear dipole interaction.

We suggest that these methods will find application in the development of solid-state quantum computing. In analogy to an actuator, modulations of the electron spin in turn modulate the anisotropic hyperfine interactions, thus generating quantum gates between nuclear spins while leaving the final state of the electron identical to its initial state. Previously studied solid-state spin systems with multiple resolved nuclear spins [4,8–10,32] can thus be controlled by only

modulating the electron spin states. Moreover, one can augment the controllable Hilbert space by coupling localized multiple electron spin states. Such coupling may be electrical, with systems such as phosphorous-doped silicon or optical in systems akin to nitrogen-vacancy defects in diamond [33]. As the ultimate utility of these systems depends on their decoherence, characterization of these mechanisms is key. Precise unitary engineering can also be used to measure relaxation processes or perform quantum process tomography in hyperfine coupled systems [25].

We thank Colm Ryan for providing his implementation of the GRAPE algorithm and Peter Allen for technical assistance in the experimental setup. We also thank Navin Khaneja for useful discussions; he recently provided a similar construction for control [34]. This work was supported in part by the National Security Agency (NSA) under Army Research Office (ARO) Contract Nos. DAAD190310125 and W911NF-05-1-0459 and by DARPA. J.C.Y. acknowledges support from the Army Research Office (ARO).

- 
- [1] B. E. Kane, *Nature (London)* **393**, 133 (1998).  
 [2] D. Loss and D. P. DiVincenzo, *Phys. Rev. A* **57**, 120 (1998).  
 [3] M. Mehring, J. Mende, and W. Scherer, *Phys. Rev. Lett.* **90**, 153001 (2003).  
 [4] M. Mehring and J. Mende, *Phys. Rev. A* **73**, 052303 (2006).  
 [5] A. M. Tyryshkin, J. J. L. Morton, S. C. Benjamin, A. Ardavan, G. A. D. Briggs, J. W. Ager, and S. A. Lyon, *J. Phys.: Condens. Matter* **18**, S783 (2006).  
 [6] M. Mehring, W. Scherer, and A. Weidinger, *Phys. Rev. Lett.* **93**, 206603 (2004).  
 [7] J. J. L. Morton, A. M. Tyryshkin, A. Ardavan, S. C. Benjamin, K. Porfyraakis, S. A. Lyon, and G. A. D. Briggs, *Nat. Phys.* **2**, 40 (2006).  
 [8] F. Jelezko, T. Gaebel, I. Popa, M. Domhan, A. Gruber, and J. Wrachtrup, *Phys. Rev. Lett.* **93**, 130501 (2004).  
 [9] L. Childress, M. V. G. Dutt, J. M. Taylor, A. S. Zibrov, F. Jelezko, J. Wrachtrup, P. R. Hemmer, and M. D. Lukin, *Science* **314**, 281 (2006).  
 [10] M. V. G. Dutt, L. Childress, L. Jiang, E. Togan, J. Maze, F. Jelezko, A. S. Zibrov, P. R. Hemmer, and M. D. Lukin, *Science* **316**, 1312 (2007).  
 [11] R. Hanson, F. M. Mendoza, R. J. Epstein, and D. D. Awschalom, *Phys. Rev. Lett.* **97**, 087601 (2006).  
 [12] E. C. Hoffmann, M. Hubrich, and A. Schweiger, *J. Magn. Reson., Ser. A* **117**, 16 (1995).  
 [13] A. Ponti and A. Schweiger, *J. Chem. Phys.* **102**, 5207 (1995).  
 [14] S. Lloyd, *Phys. Rev. A* **62**, 022108 (2000).  
 [15] A. Schweiger and G. Jeschke, *Principles of Pulse Electron Paramagnetic Resonance* (Oxford University Press, New York 2001).  
 [16] The relative order of terms for  $\mathcal{H}_0$  to hold is  $\beta_e \|g_{\mu z}\| B_0 \gg \|\gamma_n(1-\delta)B_0\| \sim \|A_{z\nu}\| \gg \|D^{j,k}\|$ .  
 [17] V. Ramakrishna, M. V. Salapaka, M. Dahleh, H. Rabitz, and A. Peirce, *Phys. Rev. A* **51**, 960 (1995).  
 [18] S. G. Schirmer, H. Fu, and A. I. Solomon, *Phys. Rev. A* **63**, 063410 (2001).  
 [19] C. Altafini, *J. Math. Phys.* **43**, 2051 (2002).  
 [20] G. Turinici and H. Rabitz, *Chem. Phys.* **267**, 1 (2001).  
 [21] N. Khaneja, T. Reiss, C. Kehlet, T. Schulte-Herbrüggen, and S. J. Glaser, *J. Magn. Reson.* **172**, 296 (2005).  
 [22] E. Fortunato, M. Pravia, N. Boulant, G. Teklemariam, T. Havel, and D. G. Cory, *J. Chem. Phys.* **116**, 7599 (2002).  
 [23] J. Baugh, O. Moussa, C. A. Ryan, A. Nayak, and R. Laflamme, *Nature (London)* **438**, 470 (2005).  
 [24] For organic crystal systems of a few nuclear spins the values of the hyperfine interaction are tens of MHz as are the Rabi frequencies for pulsed electron spin resonance (ESR) [15,25,26], while the nuclear Rabi frequency is at most 1 MHz [27]. The nuclear-nuclear dipolar coupling is tens of kHz. The quantum gate times are inversely proportional to the interaction strength.  
 [25] S. Lee, B. R. Patyal, and J. H. Freed, *J. Chem. Phys.* **98**, 3665 (1993).  
 [26] R. Rakhmatullin, E. Hoffmann, G. Jeschke, and A. Schweiger, *Phys. Rev. A* **57**, 3775 (1998).  
 [27] K. Yamauchi, J. W. G. Janssen, and A. P. M. Kentgens, *J. Magn. Reson.* **167**, 87 (2004).  
 [28] N. F. Ramsey, *Phys. Rev.* **78**, 695 (1950).  
 [29] R. C. McCalley and A. L. Kwiram, *J. Phys. Chem.* **97**, 2888 (1993).  
 [30]  $U_{jk}(\theta) = e^{[-i(\theta/2)\sigma_x^{jk}]}$ . The operator  $\sigma_x^{jk} = |j\rangle\langle k| + |k\rangle\langle j|$ .  
 [31] See EPAPS Document No. E-PLRAAN-77-R11806 for a description of this gate. For more information on EPAPS, see <http://www.aip.org/pubservs/epaps.html>.  
 [32] F. Jelezko, T. Gaebel, I. Popa, A. Gruber, and J. Wrachtrup, *Phys. Rev. Lett.* **92**, 076401 (2004).  
 [33] L. I. Childress, J. M. Taylor, A. Sorensen, and M. D. Lukin, *Phys. Rev. A* **72**, 052330 (2005).  
 [34] N. Khaneja, *Phys. Rev. A* **76**, 032326 (2007).